# Pentapeptide-rich peptidoglycan at the Bacillus subtilis cell-division site

Morales Angeles, Danae; Liu, Yun; Hartman, Alwin M; Borisova, Marina; de Sousa Borges, Anabela; de Kok, Niels; Beilharz, Katrin; Veening, Jan-Willem; Mayer, Christoph; Hirsch, Anna K H

*Published in:*
Molecular Microbiology

*DOI:*
10.1111/mmi.13629



*Publication date:*
2017

Molecular Microbiology (2017) 104(2), 319–333

doi:10.1111/mmi.13629
First published online 6 February 2017

# Pentapeptide-rich peptidoglycan at the *Bacillus subtilis* cell-division site

**Danae Morales Angeles,[1] Yun Liu,[2] Alwin M. Hartman,[2] Marina Borisova,[3] Anabela de Sousa Borges,[1] Niels de Kok,[1] Katrin Beilharz,[4] Jan-Willem Veening,[4,5] Christoph Mayer,[3] Anna K.H. Hirsch[2] and Dirk-Jan Scheffers[1]***

[1]*Department of Molecular Microbiology, Groningen Biomolecular Sciences and Biotechnology Institute University of Groningen, The Netherlands.*
[2]*Stratingh Institute for Chemistry, University of Groningen, The Netherlands.*
[3]*Department of Biology, Interfaculty Institute of Microbiology and Infection Medicine Tübingen, University of Tübingen, Tübingen, Germany.*
[4]*Molecular Genetics Group, Groningen Biomolecular Sciences and Biotechnology Institute, Centre for Synthetic Biology, University of Groningen, The Netherlands.*
[5]*Department of Fundamental Microbiology, Faculty of Biology and Medicine, University of Lausanne, Biophore Building, Lausanne CH-1015, Switzerland.*

## Summary

**Peptidoglycan (PG), the major component of the bacterial cell wall, is one large macromolecule. To allow for the different curvatures of PG at cell poles and division sites, there must be local differences in PG architecture and eventually also chemistry. Here we report such local differences in the Gram-positive rod-shaped model organism *Bacillus subtilis*. Single-cell analysis after antibiotic treatment and labeling of the cell wall with a fluorescent analogue of vancomycin or the fluorescent D-amino acid analogue (FDAA) HCC-amino-D-alanine revealed that PG at the septum contains muropeptides with unprocessed stem peptides (pentapeptides). Whereas these pentapeptides are normally shortened after incorporation into PG, this activity is reduced at division sites indicating either a lower local degree of PG crosslinking or a difference in PG composition, which could be a topological marker for other proteins. The pentapeptides remain partially unprocessed after division when they form the new pole of a cell. The accumulation of unprocessed PG at the division site is not caused by the activity of the cell division specific penicillin-binding protein 2B. To our knowledge, this is the first indication of local differences in the chemical composition of PG in Gram-positive bacteria.**

Accepted 18 January, 2017. *For correspondence. E-mail d.j.scheffers@rug.nl; Tel. +31-50-3632319; Fax +31-50-3632154.



## Introduction

The bacterial cell wall is a structure unique to bacteria, providing shape and protection from environmental challenges to the cell. The main component of the cell wall is peptidoglycan (PG). PG is a large macromolecule composed of glycan strands connected by peptide cross-bridges that form a net-like structure (Typas *et al.*, 2012; Turner *et al.*, 2014; de Pedro and Cava, 2015; Randich and Brun, 2015). Isolated PG molecules, so-called sacculi, retain the shape of the cell they surrounded (Höltje, 1998). PG is constantly remodeled to allow the bacterial cell to expand its volume, to divide, and to allow the attachment of other molecules such as teichoic acid, or to allow the incorporation of proteins that cross the PG layer (e.g., pili, flagella) (Höltje, 1998). PG grows by the incorporation of LipidII precursor molecules, composed of a disaccharide with a pentapeptide side chain, connected to a bactoprenol carrier molecule that anchors the building block to the membrane. The disaccharide moiety is coupled to a glycan strand by a glycosyl transferase and released from the carrier, and the pentapeptide moiety can be crosslinked to peptides on different strands by transpeptidases.

The pentapeptide composition differs between bacteria, for instance in *Bacillus subtilis* the pentapeptide is composed of L-Ala-D-Glu-L-meso-diaminopimelic acid-D-Ala-D-Ala, but the method of the primary DD-crosslink formation is very similar: the D-amino acid on the 4th position of one pentapeptide is covalently attached to the crosslinking protein (a transpeptidase), with concurrent release of the 5th D-amino acid on the pentapeptide. The donor peptide is subsequently crosslinked to the 3rd amino acid on the acceptor pentapeptide,

generally an amino acid containing a free amino group, such as meso-diaminopimelic acid or L-lysine. Additionally, L,D-crosslinks can be formed between two amino acids at position 3, although these crosslinks are neither universal nor do they appear to be essential (Magnet *et al.*, 2008; Cava *et al.*, 2011). Not all peptides are used in crosslinks, and unlinked pentapeptides are generally modified to tetra- or tripeptides, except in some bacteria such as *Staphylococcus aureus* that contains a very large amount of free pentapeptides (de Jonge *et al.*, 1992). In *S. aureus*, the degree of PG crosslinking is a determinant for antibiotic resistance, with lower crosslinking resulting in higher antibiotic sensitivity (Memmi *et al.*, 2008), through a yet unknown mechanism, which may have to do with easier access to the antibiotic target, or an overall weaker PG structure.

PG is one large molecule, and its synthesis and turnover are controlled by a large group of enzymes that coordinate these activities on various locations along the bacterial cell wall. In rod-shaped bacteria, two complexes for PG synthesis have been identified, the 'elongasome' and the 'divisome', responsible for PG synthesis along the lateral wall and at the cell division site respectively (Typas *et al.*, 2012; Szwedziak and Lowe, 2013; Randich and Brun, 2015). These two machines are coordinated by the cytoskeletal proteins MreB and FtsZ and consist of LipidII synthetases, flippases, membrane proteins with unknown coordinating functions such as MreC/D and RodZ, proteins from the Shape, Elongation, Division and Sporulation (SEDS) family and Penicillin Binding Proteins (PBPs). SEDS and PBPs are the proteins that incorporate LipidII molecules into PG. SEDS proteins, such as FtsW and RodA, have glycosyl transferase activity (Cho *et al.*, 2016; Meeske *et al.*, 2016). PBPs are divided into two groups: high-molecular-weight (HMW) and low-molecular-weight (LMW) PBPs. HMW PBPs are further classified into class A PBPs, whose members show glycosyl transferase and transpeptidation activity, and class B PBPs, whose members only have transpeptidation activity. The LMW PBPs have various activities, such as DD-carboxypeptidase, transpeptidase or endopeptidase activity, but always one activity per enzyme (Scheffers and Pinho, 2005).

The different machineries involved in PG synthesis and the different structural requirements to PG on different locations in the cell, suggest that the composition of PG may vary along the sacculus. Atomic force microscopy showed that there are local differences in PG architecture between division sites and other places along the bacterial wall, which vary in thickness or in patterning (Hayhurst *et al.*, 2008; Turner *et al.*, 2014). However, this technique does not reveal the underlying chemistry or crosslinking degree. Fluorescent labeling methods have uncovered different PG growth modes used by different bacteria (Kuru *et al.*, 2012; Typas *et al.*, 2012; Pinho *et al.*, 2013; Cameron *et al.*, 2015), yet what happens after the insertion of LipidII is unclear. Currently, local modifications to PG and local changes to the crosslinking degree cannot be identified as the methods to analyze PG composition provide only information on population averages (Turner *et al.*, 2014).

In this study, we use a combination of antibiotics treatment and labeling of the cell wall with a fluorescent analogue of vancomycin (Van-FL) or the fluorescent D-amino acid analogue (FDAA) HCC-amino-D-alanine (HADA). Van-FL binds to the terminal D-Ala-D-Ala of the disaccharide pentapeptide subunit (Daniel and Errington, 2003), whereas HADA is incorporated at the 5th position in *Bacillus subtilis* stem-peptides and rapidly processed after incorporation (Kuru *et al.*, 2012), so both labeling methods only reveal unincorporated LipidII and newly synthesized PG. We found that septal PG is rich in pentapeptides, and that these pentapeptides remain partially unprocessed after division when they form the new pole of a cell. Mature PG contains only a small number of pentapeptides, 3.7% of total muropeptides of which 1.6% contains a terminal D-Ala and 2.1% a glycine residue at position 5 (Atrih *et al.*, 1999). This is the first indication of local differences in the chemical composition of PG in Gram-positive bacteria. Our findings reveal that there are local differences in PG crosslinking and processing throughout the cell wall.

## Results

### *PG at the division site contains high concentrations of pentapeptides*

We used fosfomycin to block LipidII synthesis, and then stained nascent PG with Van-FL. To our surprise, 20 min treatment with fosfomycin at a concentration that blocks synthesis of new LipidII and PG (Dominguez-Escobar *et al.*, 2011; Garner *et al.*, 2011), does not completely block Van-FL labeling of cells (Fig. 1A), something that would be expected if Van-FL predominantly labels LipidII. Daniel and Errington (Daniel and Errington, 2003) also observed continued Van-FL labeling of cells that were treated with various antibiotics that block LipidII synthesis, and interpreted this as an incomplete block of LipidII synthesis. Bacitracin treatment had a stronger effect on reduction of Van-FL staining than fosfomycin (Daniel and Errington, 2003). We decided to investigate this phenomenon in more detail, using both Van-FL and the newly developed D-Ala analogue HADA, which in *B. subtilis* is incorporated exclusively in the 5th position of the stem peptide (Kuru *et al.*, 2012) (Supporting Information Fig. S1). Van-FL and HADA labeling

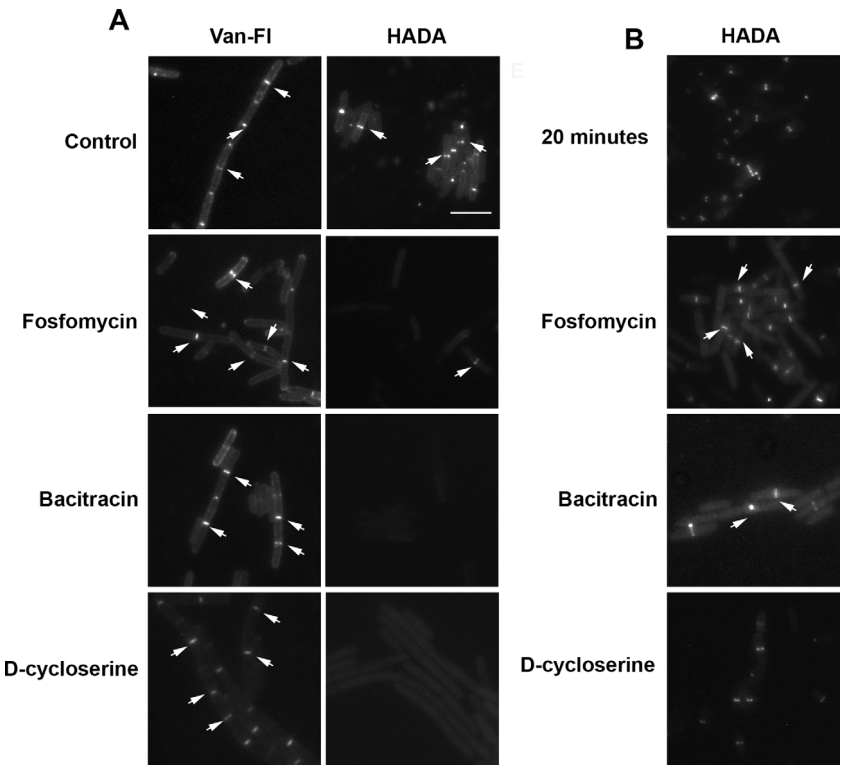


**Fig. 1.** Accumulation of unprocessed pentapeptides at the septum. Exponentially growing *B. subtilis* (168) was either labeled with Van-Fl or HADA after growth for 20 min in the absence (control) or presence of fosfomycin (500 μg/ml) bacitracin (500 μg/ml) or D-cycloserine (500 μg/ml) to block LipidII synthesis (A). In a reverse experiment, cells were labeled with HADA for 5 min and allowed to continue growth for 20 min in the presence of fosfomycin or bacitracin (B). Arrows indicate labeled septa. Scale bar (same for all): 5 μm.

both report the presence of a pentapeptide, but Van-FL can label pentapeptides that are already present before the label is added, whereas HADA labeling depends on active LipidII/PG synthesis.

*B. subtilis* grown in the presence of either fosfomycin, bacitracin or D-cycloserine for 20 min prior to labeling with Van-FL, showed strong labeling at the division site (Fig. 1A). None of these treatments killed the cells within the 20 min timeframe of the experiment as determined by both membrane permeability measurements as well as dilutions of treated cells, although prolonged exposure (60 min) did have an effect (Supporting Information Table S1, Fig. S2). Quantification of the fluorescence signals at the septum revealed that fluorescence was increased when cells were treated with fosfomycin and bacitracin, but not when cells were treated with D-cycloserine (Supporting Information Fig. S3). We cannot explain the increase in Van-FL signal but do note that also the background signal was higher in the fosfomycin and bacitracin stained samples. There are various possible explanations for the septal labeling pattern, which could also occur in combinations. First, if the antibiotic-induced block of LipidII synthesis is incomplete, this could cause accumulation of LipidII. Second, LipidII at the division site may no longer be incorporated into PG and/or processed during the 20 min period in which PG synthesis is blocked. Third, bacitracin and fosfomycin inhibit the activity of carboxypeptidases that cleave D-Ala at position 5. Fourth, Van-FL could label existing PG material, not LipidII, of which the pentapeptide has not been processed as the donor in crosslinking or through cleavage of the 5th D-Ala. To distinguish between these explanations, we repeated the experiment with HADA labeling. Fosfomycin treatment resulted in a near complete block of HADA incorporation, and bacitracin and D-cycloserine completely abolished HADA incorporation (Fig. 1A), indicating that, in fact, the antibiotic treatments efficiently block LipidII synthesis. This result strongly suggests that the Van-FL label observed at the division site is not caused by the staining of residual LipidII that was synthesized during the antibiotic treatment. Then, in a reverse experiment, cells were labeled with HADA before resuspension in growth medium for 20 min in the presence of fosfomycin, bacitracin or D-cycloserine. Cells treated in this manner showed strong division-site labeling, similar to the Van-FL labeling (Fig. 1B), indicating that HADA is incorporated into the cell wall, but then fails to be processed at the division site. HADA labeling followed by 20 min of growth without antibiotics also resulted in septal labeling, indicating that the retention of label is not the result of blocked PG synthesis or processing (Fig. 1B top panel). Comparison of the level of HADA fluorescence at the septa indicated that the levels of fluorescence were similar for all cells analyzed (Supporting Information Fig. S3).

Kuru *et al.* (2012) used a *B. subtilis dacA* (PBP5) knockout strain to visualize PG along the lateral wall. PBP5 is the major D,D-carboxypeptidase of *B. subtilis* which contributes to PG maturation by removing the majority of terminal D-Ala residues from stem peptides that were not used as donors in crosslinking reactions (Atrih *et al.*, 1999). We repeated the labeling experiments in a *dacA* knockout strain, to see if we could increase the labeling, especially at the lateral wall. As expected, both HADA and Van-FL labeling at the lateral wall increased due to the increase of unprocessed pentapeptides in PG (Fig. 2A and D). Van-FL labeled the entire cell circumference, which can be explained by the fact that Van-FL labels all D-Ala-D-Ala residues in the wall. HADA resulted in a patchy pattern on the lateral wall, as it is only labeling material synthesized during the 5 min labeling pulse. Blocking PG synthesis with bacitracin, again almost completely blocked HADA incorporation all over the cells (Fig. 2B), whereas Van-FL still labeled the cell circumference (Fig. 2E), indicating that this labeling pattern reflected primarily PG, not LipidII. Again, when cells were labeled with HADA before blocking PG synthesis, label was retained at the division site, indicative of absence of processing at the division site (Fig. 2C).

It has been reported that in some bacteria the incorporation of fluorescent D-amino acids occurs primarily through exchange reactions on the outside of the cell, and thus that the FDAA is not incorporated into LipidII itself (Kuru *et al.*, 2012; Tsui *et al.*, 2014). In *B. subtilis*, the major PBP responsible for such an exchange reaction is PBP4, in the absence of which incorporation of various NBD-labeled D-amino acid analogues is reduced but not blocked (Fura *et al.*, 2015). We confirmed that this was the same for HADA-labeling: although overall labeling was somewhat reduced in a PBP4 knockout strain, septal labeling was still clearly detectable (Supporting Information Fig. S4). Treatment of cells with D-cycloserine, which blocks incorporation of D-Ala into LipidII, completely blocked HADA-labeling of cells (Fig. 1A). Fosfomycin, which blocks LipidII synthesis but not transpeptidase activity, causes a block of HADA labeling in *B. subtilis* (Fig. 1A). In *Escherichia coli*, where all incorporation occurs via transpeptidation (Kuru *et al.*, 2012, 2015), cells could still be labeled with HADA after a 20 min treatment with fosfomycin (Supporting Information Fig. S5). Finally, our results in *B. subtilis* 168 were not strain-specific as HADA labeling of strain PY79 gave similar results (Supporting Information Fig. S5). Combined, these controls suggest that at least part of the HADA-labeling in *B. subtilis* occurs via the LipidII route.

### *Division-site labeling is caused by accumulated pentapeptides, not unincorporated LipidII*

Although the above results indicate that it is unlikely that the Van-FL/HADA fluorescence observed at the division site is produced by an accumulation of LipidII, we wanted to confirm that the labeling pattern reflects material that has been incorporated into PG. To do so, we isolated sacculi from HADA-labeled and non-labeled cells. The isolation of sacculi involves boiling the cells repeatedly in

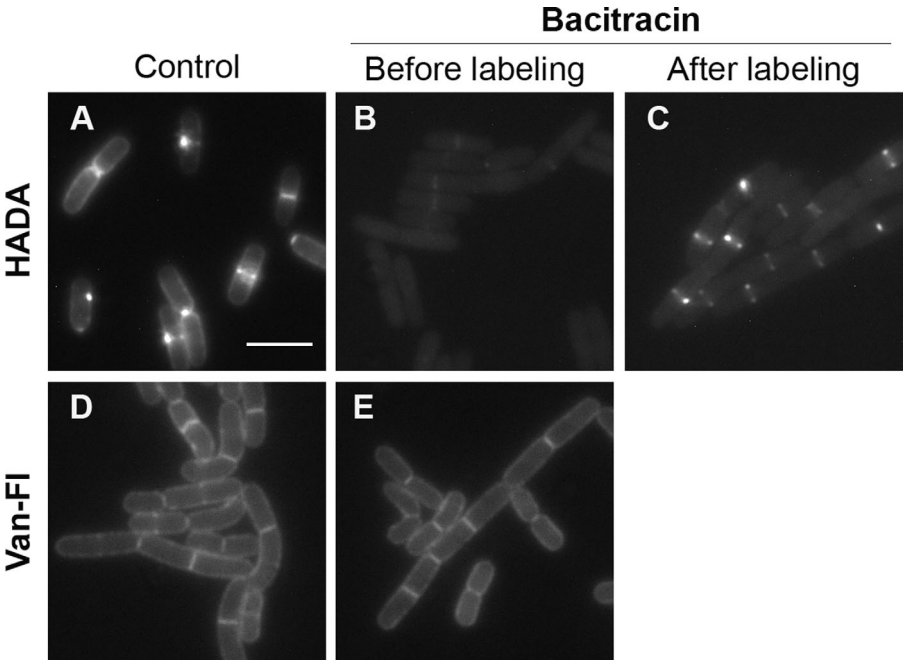


**Fig. 2.** Accumulation of pentapeptides at the septa of a *dacA* knockout strain. Exponentially growing *B. subtilis* 4056 was either labeled with HADA (A, B) or Van-Fl (D, E) after growth for 20 min in the absence (A,D) or presence of bacitracin (500 μg/ml, B,E) to block LipidII synthesis. In a reverse experiment, cells were labeled with HADA and allowed to continue growth for 20 min in the presence of bacitracin (C). Scale bar (same for all): 5 μm.

SDS and treatment with hydrofluoric acid, which should remove all membrane associated LipidII and wall-associated polysaccharides. Sacculi isolated from HADA-labeled cells displayed clear HADA labeling in rings at the division sites, indicative of PG with a high concentration of pentapeptides at the division site (Fig. 3A). Sacculi isolated from non-labeled cells, which were subsequently labeled with Van-FL displayed a similar labeling pattern (Fig. 3B), although in addition to division rings, polar fluorescence was also occasionally detected. Sacculi were also isolated from cells that were grown for 20 min in the presence of bacitracin, fosfomycin or D-cycloserine. When these sacculi were labeled with Van-FL similar patterns were observed as for the cells grown in the absence of antibiotics (Fig. 3D, F, and H). Finally, sacculi isolated from cells that were HADA-labeled and then grown for an additional 20 min in the presence of bacitracin, fosfomycin or D-cycloserine also still showed rings (Fig. 3C, E, G). This result shows that the accumulation of pentapeptide material at the septum is not caused by an accumulation of LipidII or the result of antibiotic treatment. As a final control for HADA incorporation into PG, HADA-labeled sacculi were incubated with lysozyme and the fluorescence was followed over time (Fig. 4). Lysozyme digests the 1,4-β-glycosidic bond between MurNAc and GlcNAc, therefore if the fluorescence is caused by HADA that is incorporated into PG, the signal at the septum should decrease over time as PG fragments are released by lysozyme. Lysozyme digestion was followed for 10 min, with an untreated sample as a control for bleaching. The fluorescence at the division site of the sacculi treated with lysozyme decreased over time, compared to the untreated control (Fig. 4, compare signals at arrows between top and bottom rows). Combined, these results show that the HADA-label is incorporated into the PG and that there is an accumulation of unprocessed D-Ala-D-Ala at division sites.

### *3D structure of the pentapeptide rings*

To visualize the 3D structure of the pentapeptide containing PG at the division site in live cells, Z-stack pictures of HADA-labeled *B. subtilis* in exponential phase were taken, followed by deconvolution and 3D reconstruction. Figure 5 shows that the labeled muropeptides at the division site form a structure similar to a ring, comparable to what was observed with sacculi (Fig. 3). This kind of donut-shaped ring structure also looks like the structure of the *B. subtilis* septum obtained with atomic force microscopy (Hayhurst *et al*., 2008). In addition, Kuru *et al*. showed that *E. coli*, *Agrobacterium tumefaciens* and *S. aureus* also present a ring at the division site when labeled with a short HADA pulse (2012).

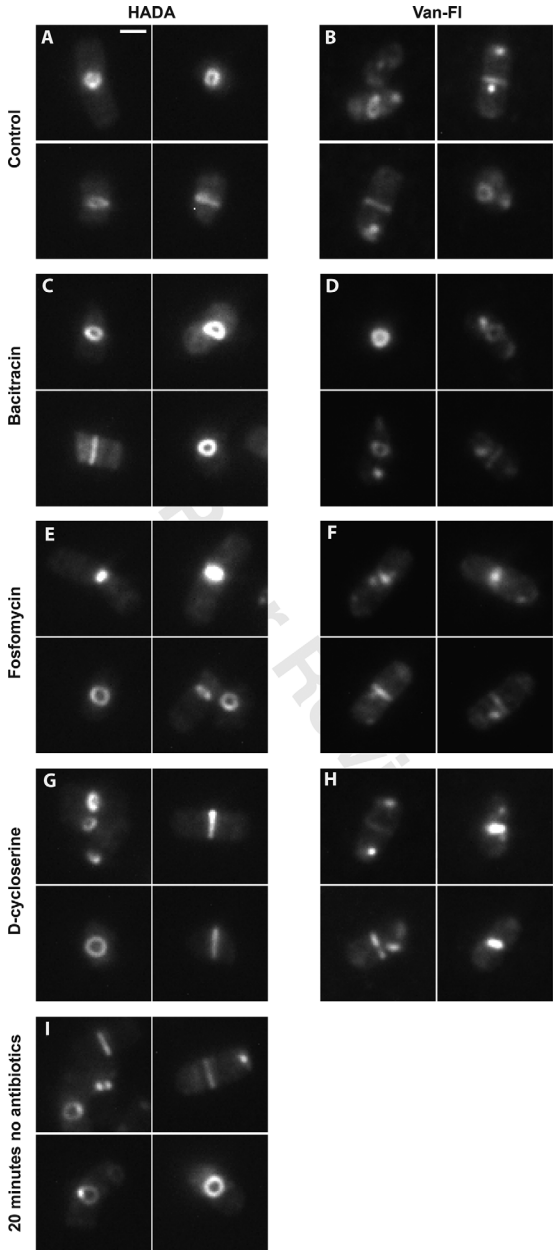


**Fig. 3.** Pentapeptides are present at the septum in isolated sacculi. Exponentially growing *B. subtilis* were labeled with HADA and sacculi were isolated from labeled and non-labeled cells either immediately (A–B) or after 20 min of continued growth in the presence of bacitracin (500 μg/ml C–D), fosfomycin (500 μg/ml E–F), D-cycloserine (500 μg/ml G-H) or without antibiotic (I). After isolation, sacculi were stained with Van-FL (B, D, F, H). HADA fluorescence (A, C, E, G, I) Van-FL fluorescence (B, D, F, H) Scale bar (same for all): 1 μm.

### *Pentapeptides at the division sites are retained at the poles and eventually processed*

We used fluorescence time-lapse microscopy to determine if the pentapeptide-enriched PG at the septum is processed. Exponentially growing *B. subtilis* cells were

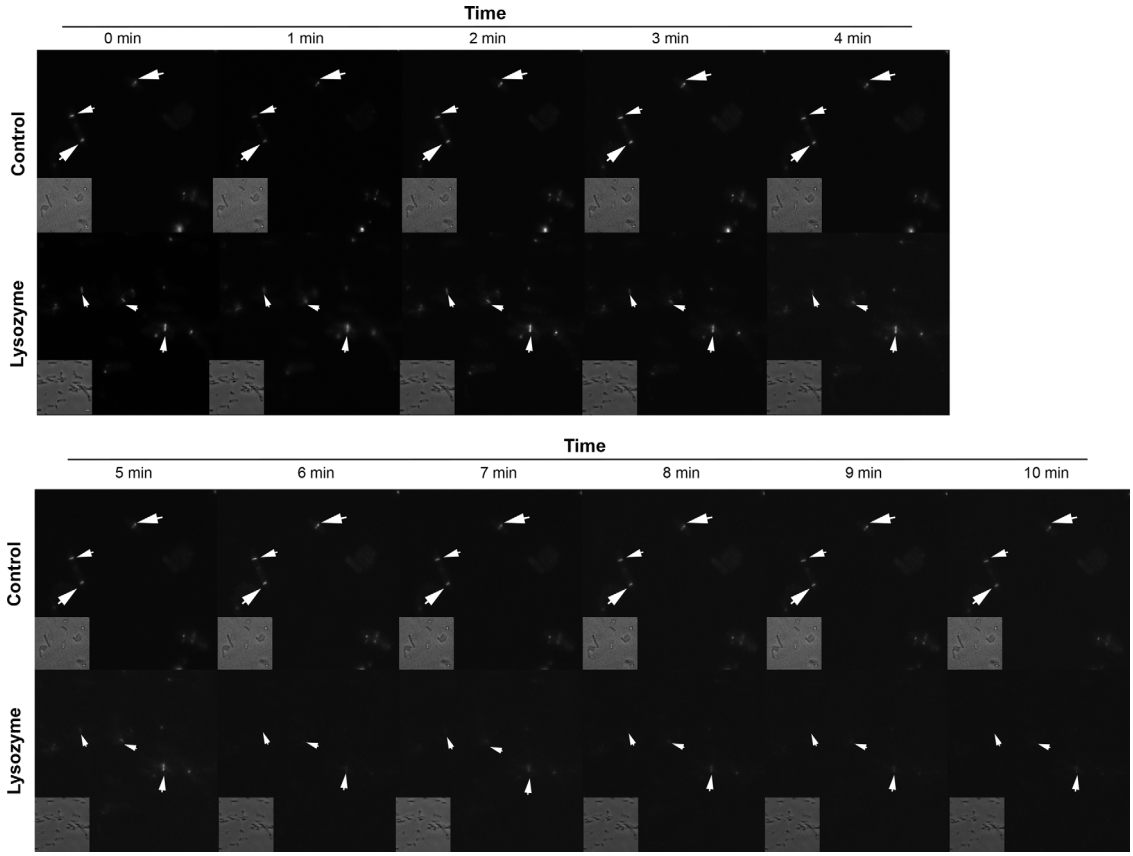


**Fig. 4.** Lysozyme digestion of HADA-labeled PG. HADA-labeled sacculi were applied to agarose slides (control, top row) or to agarose slides impregnated with lysozyme (lysozyme, bottom row) and imaged every 10 min. Inserts at left bottom show phase contrast images taken simultaneous with the fluorescence image to confirm the presence and retention of sacculi on the agarose pads. Arrows indicate labeled septa, which clearly persist in the control sample, compared to the disappearance of label from the lysozyme treated samples.

labeled with a short pulse of HADA, and *B. subtilis* growth was followed by fluorescence time-lapse microscopy (Fig. 6). At the initial stage, HADA labeling is localized as a band at the septum and the signal stays strong in agreement with our previous results. As the size of the cells increases and the septum starts to become two new poles, the HADA signal decreases indicating that some HADA-labeled material is processed. Interestingly, after the cells have split, some HADA signal is retained in both new cells at the poles, suggesting that crosslinked muropeptides containing HADA are integrated to the cell wall at the poles. Fluorescence at the poles was also conserved in the next generation. These results are similar to those obtained with *E. coli* by de Pedro *et al.* (1997), confirming that the material incorporated into the poles is highly stable, and to a recent study from the Winkler lab where retention of HADA at cell poles was observed (Boersma *et al.*, 2015).

Next, we investigated whether it was possible to increase polar HADA labeling. Deletion of both *ezrA* and *gpsB* has been reported to lead to polar retention of PBP1 and ongoing polar PG synthesis as reported by Van-FL staining (Claessen *et al.*, 2008). Van-FL labeling of *ezrA gpsB* double mutant cells indeed resulted in fluorescent labeling of the cell poles, as expected (Fig. 7) and was not observed with the single deletions as reported (not shown). However, with HADA no polar labeling was observed (Fig 7). We confirmed this observation by analyzing the fluorescence distribution along the length of the cell which showed that cells labeled with Van-FL have increased labeling at the poles which is completely absent from HADA-labeled cells, whereas increased labeling at division septa and at 1/4 and 3/4 positions along the length of the cells was observed with both labeling methods (Fig. 7). As HADA labeling requires active PG synthesis this result strongly suggests that it takes cells longer to process pentapeptides present in polar PG in the absence of *ezrA* and *gpsB*, but also that the polar Van-FL labeling is not the result of ongoing synthesis at the poles. In addition, this result (together with those from the *dacA* mutant, Fig. 2) shows that in the absence of antibiotics, it is possible to obtain different labeling patterns for Van-FL and HADA.

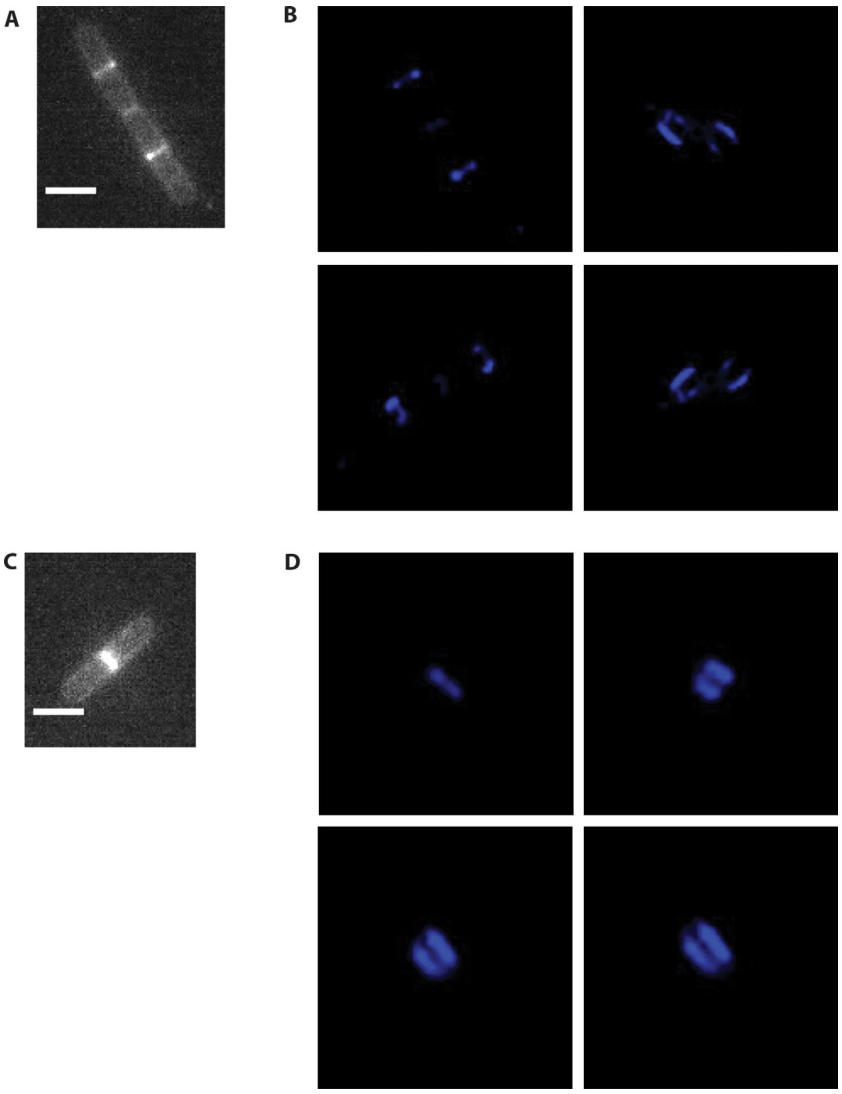


**Fig. 5.** 3D reconstruction of HADA-labeled septa. Cells were imaged along the *Z*-axis resulting in image stacks (A, C) from which 3D reconstructions (B, D) were made using Deltavision software. B and D show different angles of the reconstructions, which can be viewed in Supporting Information Movies S1 and S2. Scale bar: 2 μm.

Again, this indicates that Van-FL labels existing pentapeptides whereas HADA only reports on newly synthesized pentapeptides.

### *Pentapeptides at the septum are not involved in PBP2B localization*

Cell division requires the activity of a specific Class B transpeptidase, PBP2B in *B. subtilis* (Daniel *et al.*, 1996). Presence of this protein is essential for division and in its absence other cell division proteins, collectively known as the divisome, also lose their localization at the division site (Daniel *et al.*, 2000). PBP2x, the PBP2B homologue of *Streptococcus pneumoniae*, is required for labeling of the constricting septa with FDAAs (Tsui *et al.*, 2014). In addition, the localization of PBP2x to midcell is dependent on its PASTA domains (Peters *et al.*, 2014). PASTA domains are capable of binding uncrosslinked muropeptides albeit with low (millimolar) affinity (Shah *et al.*, 2008; Paracuellos *et al.*, 2010; Maestro *et al.*, 2011; Mir *et al.*, 2011; Squeglia *et al.*, 2011; Peters *et al.*, 2014). We wanted to investigate whether the cell-division-specific activity of PBP2B, which contains two C-terminal PASTA domains, is responsible for generating the pentapeptide-enriched PG at the septum, and/or whether the PASTA domains of PBP2B are responsible for the localization of PBP2B to the septum.

GFP-PBP2B localization was not affected by bacitracin treatment, showing that a block in LipidII synthesis does not affect the assembly of the divisome (Supporting Information Fig. S6). We then generated a set of strains in which native PBP2B is produced in the presence of IPTG and GFP-PBP variants are produced in the presence of xylose (Fig. 8A). This allowed us to simultaneously check the capacity of the GFP-PBP2B

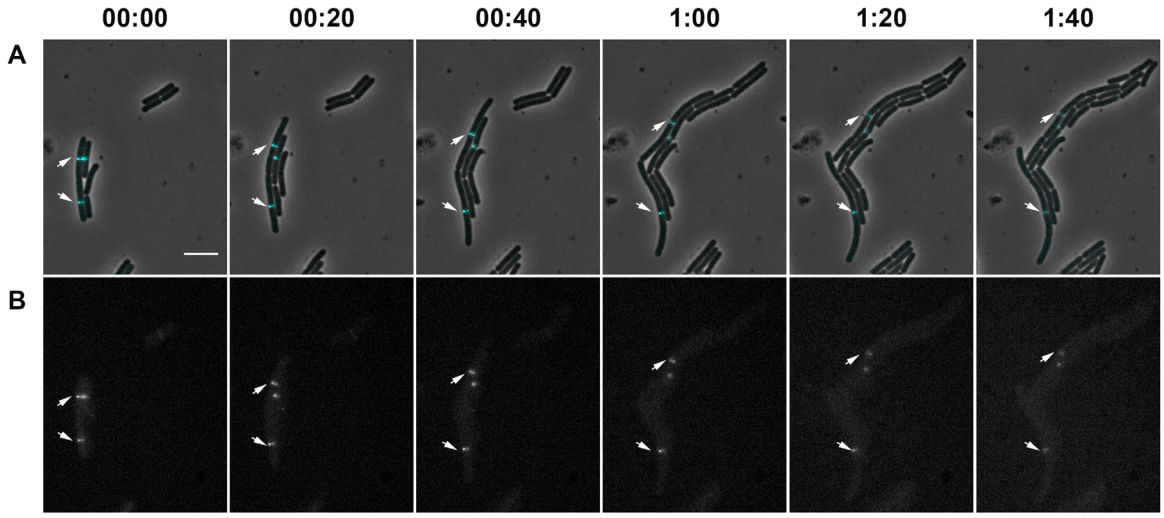


**Fig. 6.** Time-lapse of HADA labeled cells. Exponentially growing *B. subtilis* were labeled with HADA and applied to an agarose slide containing growth medium for time-lapse microscopy. The HADA signal (B) and growth of the cells (A, overlay of HADA fluorescence and phase contrast images) was imaged every 20 min for 100 min. Each arrow follows a HADA-labeled septum over time.

variants to complement the depletion of wild type PBP2B, as well as their localization. In addition to a truncation of the PASTA domains, we also created a transpeptidase-inactive mutant by changing the catalytic serine (Ser312) to alanine, and combined the catalytic site mutant with the PASTA truncation. As a control, we made a 'supertruncate' variant in which most of the PBP2B was removed.

As expected, depletion of PBP2B was lethal and expression of the GFP-supertruncate construct did not rescue this phenotype. To our surprise, all other GFP-PBP2B variants allowed cells to grow with growth rates similar to wild type GFP-PBP2B (Supporting Information Fig. S7). To make sure that the complementation was not an artifact of the GFP-fusion, a second set of strains with the *pbpB* alleles alone was created. Again, all constructs except the supertruncate complemented the depletion of *pbpB* (Supporting Information Fig. S7). The expression level of the GFP-PBP2B constructs was similar in all strains, as evidenced by the levels of in-gel GFP fluorescence. Mutation of the catalytic Ser312 was confirmed, since the active-site mutants no longer bound Bocillin-FL, which requires the catalytic serine for covalent attachment (Supporting Information Fig. S8). When we analyzed the mutant strains for localization of the GFP-PBP2B variants, we noticed that none of the

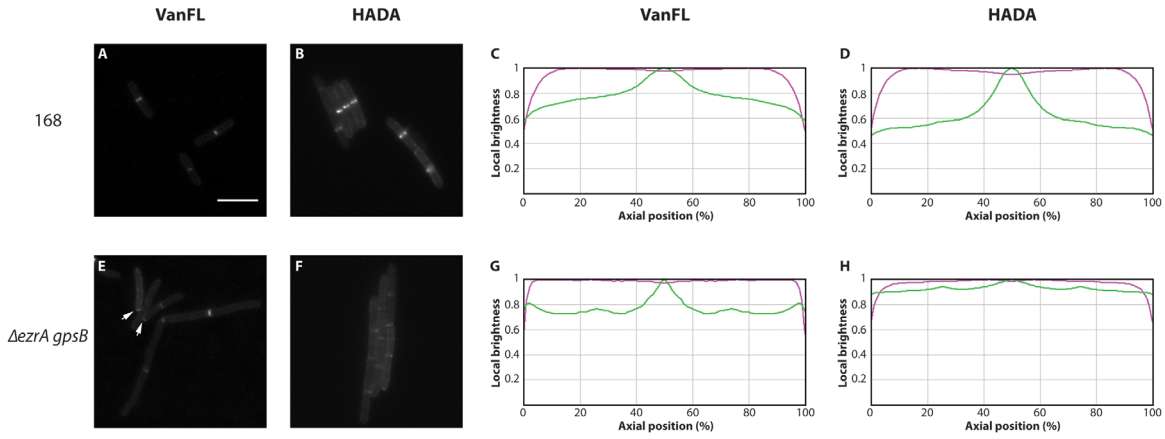


**Fig. 7.** A *gpsB ezrA* double deletion mutant does not synthesize polar PG. Exponentially growing wild type cells (168) and *gpsB ezrA* double deletion strain 4144 were labeled for 5 min with Van-Fl (A, E) or HADA (B, F) and immediately imaged. Using the ObjectJ plugin for ImageJ, the average fluorescence signal over the width of the cell was analyzed for axial positions along the length of the cell. The average signal readings were then plotted against the corresponding axial positions, resulting in a signal intensity distribution plot. Green lines represent relative fluorescence intensity, purple lines represent the relative diameter of the cell. Relative fluorescence intensities are depicted for Van-FL in wild type (C, $n = 1856$) and 4144 (G, $n = 512$) cells and HADA in wild type (D, $n = 891$) and 4144 (H, $n = 904$) cells.

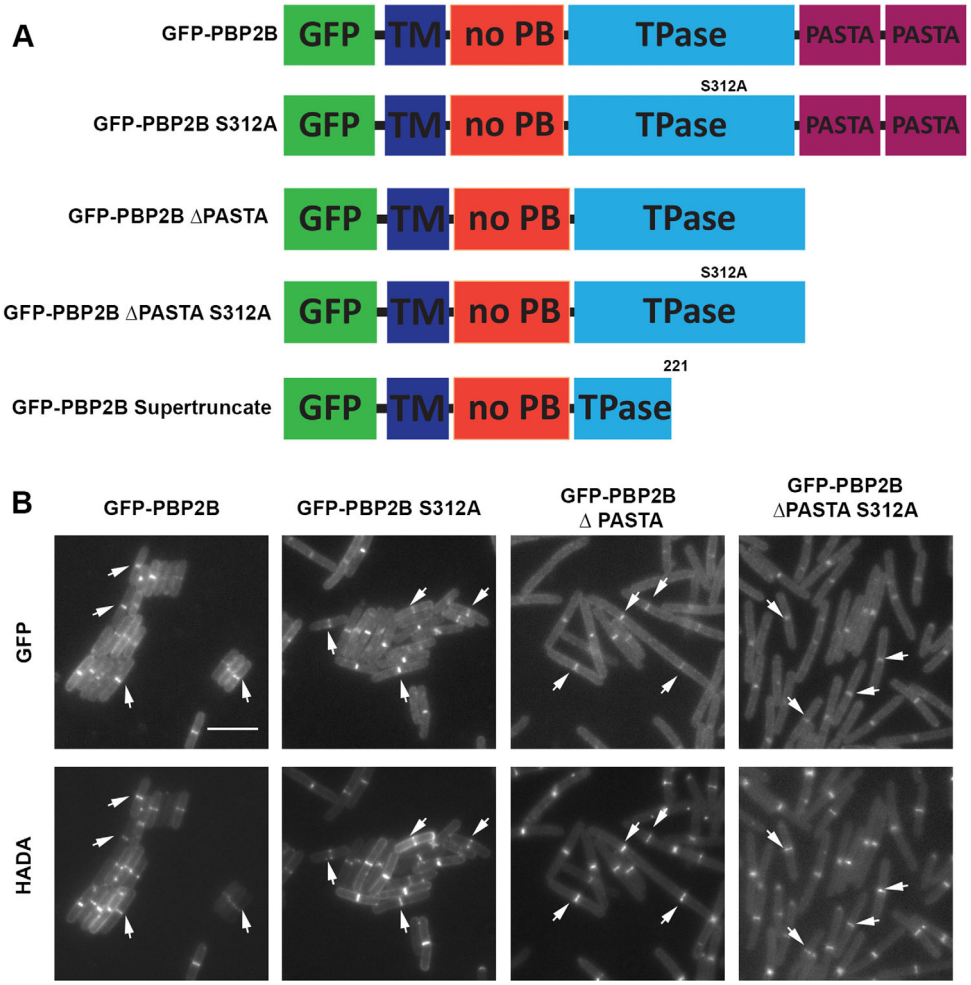


**Fig. 8.** Localization of PBP2B does not depend on PASTA domains. (A) Schematic representation of the GFP-PBP2B proteins used in this experiment. GFP – Green Fluorescent Protein; TM – transmembrane segment; no PB – non-Penicillin Binding module; TPase – transpeptidase domain; PASTA – PASTA domain. (B) Localization of GFP-PBP2B construct (top row) and cell wall synthesis imaged with HADA (bottom row) in cells depleted for wild type PBP2B, expressing (left to right) GFP-PBP2B, GFP-PBP2B S312A, GFP-PBP2B ΔPASTA and GFP-PBP2B S312A ΔPASTA. Scale bar (same for all): 5 μm.

strains showed strong cell-division defects, and that all the GFP-PBP2B variants still preferentially localized to the septum, meaning that neither the PASTA domains, nor the catalytic serine are required for PBP2B localization (Fig. 8B). Labeling of the cells with HADA revealed strong septal labeling in all cases, showing that the transpeptidase activity of PBP2B is not required for the accumulation of pentapeptide-containing PG at the septum (Fig 8B).

## Discussion

Although PG is one large macromolecule, it has long been known that there are local differences in PG architecture and possibly chemistry. The architecture of PG needs to be different to allow for the different curvatures of the sacculus at poles and division sites. Early electron microscopy studies of the *B. subtilis* cell wall have already shown wall bands at the division site (Burdett and Higgins, 1978), and different PG growth modes at the poles (Clarke-Sturman *et al.*, 1989). Atomic force microscopy revealed cable-like structures on the *B. subtilis* lateral wall and thick, defined septa (Hayhurst *et al.*, 2008). It has been well documented that next to regions of high PG turnover, there are regions of so-called inert PG (iPG) in *E. coli*, which play an important role in keeping the shape of the cells as improperly located iPG can be found at branching points in shape mutants (de Pedro *et al.*, 2003; Potluri *et al.*, 2012). Determining the underlying chemistry of local differences in PG synthesis, i.e., the level of crosslinking and processing of muropeptides at different sites in the sacculus, has so far been difficult as methods addressing these matters rely on bulk analysis of digested PG molecules by HPLC and LC/MS (Turner *et al.*, 2014). The exciting development of FDAAs to label PG synthesis (Kuru *et al.*, 2012) has made it possible to start addressing such local differences at the single-cell level.

Using the unique properties of HADA, namely its incorporation into the 5th position of the stem peptide in *B. subtilis* PG and rapid processing at the lateral wall by

PBP5 (Kuru *et al*., 2012) (Fig. 2, Supporting Information Fig. S1), we show that there is a population of stable, pentapeptide-containing PG at the division site in *B. subtilis*. The labeling patterns observed with HADA are very similar to patterns observed with Van-FL after labeling unmodified PG, and thus these patterns are truly reflective of the presence of D-Ala-D-Ala moieties at the division septum. This also explains why Van-FL labeling still reveals the division site when cell-wall synthesis is blocked with various antibiotics as shown here and by Daniel and Errington (Daniel and Errington, 2003), or when cell-wall synthesis is blocked by the addition of CCCP (Strahl *et al*., 2014), which delocalizes various proteins involved in PG synthesis such as MreB and PBP1 (Strahl and Hamoen, 2010; Lages *et al*., 2013). Importantly, the presence of pentapeptide-containing septal PG was confirmed by the observation that Van-FL labeled sacculi isolated from untreated cells at the septa. This indicates that the presence of pentapeptides at the septum is not the result of an accumulation of pentapeptides at the septum caused by HADA or Van-FL labeling of live, growing cells. Also, HADA-label was retained upon isolation of sacculi and was released by lysozyme treatment, indicating that the observed HADA-label is incorporated into PG. Some of the unprocessed PG observed at the division site is retained at the cell poles and probably part of iPG in *B. subtilis*, as was recently also noted in time-lapse experiments with *B. subtilis* PY79 where the focus was on PG turnover at the lateral wall (Boersma *et al*., 2015). However, there must be some processing of the septal material upon splitting of the cells as the label observed at the poles is never as strong as at the septum, and we also do not see consistent labeling of all poles with Van-FL. Our results suggest that PG at the poles is slowly converted into 'true' polar, inert PG, and that this processing is affected in a *ezrA gpsB* double deletion strain. This implies that PG chemistry at the pole depends on the age of the pole. Accumulation of pentapeptides at the septum has previously been proposed for *S. pneumoniae*, as its main DD-carboxypeptidase was found to be absent from the septum (Morlot *et al*., 2004), but to our knowledge, our report is the first to convincingly show the presence and persistence of pentapeptides at the septum. This does not mean that this septal material is not crosslinked, as the D-Ala-D-Ala moiety can remain attached to an acceptor stem peptide. This is also evidenced by the finding of the HADA label in the two major pentapeptide containing muropeptide peaks during HPLC analysis of a *dacA* mutant (Supporting Information Fig. S1).

PG that is incorporated at the lateral wall is processed rapidly, primarily by the major DD-carboxypeptidase PBP5. Retention of D-Ala-D-Ala containing PG at the septum thus suggests that PBP5 is absent from, or not active at the division site. A GFP-fusion to PBP5 is localized both at the septum and at the lateral wall (Scheffers *et al*., 2004), indicating that the activity of PBP5 may somehow be blocked at the division site. In *E. coli*, PBP5 and FtsZ act together (Varma and Young, 2004) and it seems to be the absence of PBP5 at mid-cell, and thus the presence of pentapeptides, that allows for a correct placement of the FtsZ-ring ensuring correct cell division and cell shape in the following generations (Potluri *et al*., 2012). *B. subtilis* does not show dramatic shape defects in the absence of DD-carboxypeptidases, but this may be because the septal PG is thick, splits rather than invaginates, and because septum shape is coordinated by other proteins that are absent from *E. coli* such as SepF (Gundogdu *et al*., 2011). How the presence of pentapeptides at the division site is communicated to FtsZ on the inside of the cell is unknown, but this may be through divisome components on either side of the membrane. A candidate protein that could connect unprocessed PG and FtsZ is PBP2B, a Class B transpeptidase that is essential for formation of the septum (Daniel *et al*., 1996, 2000), as this protein contains two PASTA domains that have been implicated in binding of uncrosslinked muropeptides (Shah *et al*., 2008; Paracuellos *et al*., 2010; Maestro *et al*., 2011; Mir *et al*., 2011; Squeglia *et al*., 2011; Peters *et al*., 2014). Recently, the localization of the essential *S. pneumoniae* PBP2x (homologue of PBP2B) was reported to be dependent on either its own C-terminal PASTA domains, or the presence of PASTA domains on its interacting partner StkP (Morlot *et al*., 2013; Peters *et al*., 2014). Removal of the PASTA domains from PBP2B did not abolish localization of PBP2B nor did it affect its function. To our surprise, replacement of the active-site serine also did not affect localization or function, and even a PBP2B construct lacking both the active site serine and the PASTA domains was functional in that it allowed cells to grow, localized to the division site and showed PG labeling similar to wild type cells. We cannot formally exclude the possibility that a minute amount of wild type PBP2B is produced in the depletion strain, which, in turn, only rescues this strain when other inactive forms of GFP-PBP2B are expressed. However, as growth rates and localization patterns of the catalytically inactive variants are indistinguishable from the wild type GFP fusion, and complementation was dependent on xylose, we deem this unlikely. Also, a construct in which most of the protein was deleted was not capable of complementing a PBP2B depletion strain. It seems that it is not the transpeptidase activity of PBP2B that is essential, but rather that the presence of the protein in the divisome is required and that its catalytic activity can be compensated by another, non-essential

transpeptidase. In this respect, it is important to note that depletion of any component of the *B. subtilis* divisome results in destabilization and delocalization of the other components (Errington *et al*., 2003).

The discovery of the accumulation of pentapeptide-containing PG may seem paradoxical as it was recently reported that proteins containing SPOR domains, that bind to 'denuded' PG, which is devoid of stem-peptides, localize to the septal site of sacculi isolated from both *B. subtilis* and *E. coli* (Yahashiri *et al*., 2015). However, it is easy to envisage that 'denuded', i.e., extremely processed, PG, and unprocessed PG coexist at the septum – while at the same time noting that we could not observe unprocessed PG in *E. coli*. In *B. subtilis*, D-Ala-D-Ala containing pentapeptides comprise only a small portion of the total PG, and even when all this material is concentrated at the septum, this would mean that a large fraction of the muropeptides at the septum are processed, for example because the stem-peptide served as a donor in a crosslinking reaction.

It remains to be established what the specific function of the pentapeptides at the septum is and how the relative lack of stem-peptide processing at the septum is regulated. We are currently investigating this.

## Experimental procedures

### *Bacterial strains and growth conditions*

Strains used in this study are listed in Table 1. All *Bacillus* strains were grown in casein hydrolysate (CH)-medium at 30°C (Anagnostopoulos and Spizizen, 1961; Harwood and Cutting, 1990). Strain 3122 was induced by adding 0.5% (w/v) xylose and strain 4055 with 0.02 mM IPTG. Strain 4056 (*dacA::kan*) was constructed by transformation of *B. subtilis* 168 with chromosomal DNA of *B. subtilis* DK654 (kind gift from Dan Kearns, Indiana University Bloomington). Deletion of *dacA* (PBP5) was confirmed by PCR and labeling with Bocillin-FL (Life-Technologies).

### *Construction of GFP-PBP2b mutants and strains*

The coding sequences for full length *pbpB* and *pbpB1-1991* were amplified from *B. subtilis* 168 chromosomal DNA using primers djs501 (5′-GTCGGATCCCTATGATTCAAAT GCCAAAAAAG) and djs502 (5′- GAACTCGAGTTAATCAG GATTTTTAAACTTAACC) or djs503 (5′- GAACTCGAGTT ATTCTTCCTTATCTGAGTCAG) respectively (503 introduces a stop codon after position 1991) and subcloned into pGEM-T (Promega). After sequencing, the PCR fragments were cloned using BamHI/XhoI into pSG1729 (Lewis and Marston, 1999), resulting in plasmids pDMA001 (*gfp-pbpB*) and pDMA002 (*gfp-pbpBΔPASTA*). pDMA001 and pDMA002 were used as template plasmids in a Quikchange PCR (Stratagene) to introduce mutation *pbpBT 934G* changing the catalytic Ser312 to Ala using primers djs504 (5′- GTATGAACCCGGGGCCACGATGAAGATC) and djs505 (5′- GATCTTCATCGTGGCCCCGGGTTCATAC) resulting in plasmids pDMA003 (*gfp-pbpBSer312Ala*) and pDMA004 (*gfp-pbpBSer312Ala-ΔPASTA*). All plasmids were sequence verified. Sequence verification of an initial PCR product generated using djs501/502 revealed the introduction of a G676A mutation resulting in a stop codon at position 222. This '*pbpB-supertruncate'* construct was subcloned into pSG1729, generating pDMA005, to serve as a negative control in complementation assays. All plasmids were cloned into *B. subtilis* 3295 and integration into the *amyE* locus was verified by growing the transformants on starch plates. To remove *gfp* from pDMA001, pDMA002, pDMA003, pDMA004 and pDMA005, these plasmids were digested using *Kpn*I and *Bam*HI. Plasmid and *gfp* DNA fragments were separated on agarose gels, plasmid DNA was isolated and the overhangs were filled using DNA Blunt enzyme (Thermo Scientific) and the linear plasmids were religated. All plasmids were sequenced and cloned into *B. subtilis* 3295 as described above.

### *Synthesis of HCC-amino-D-alanine (HADA)*

HADA synthesis was performed according to the protocol of Kuru *et al.* (2015), with details provided in the Supporting Information.

### *Inhibition of cell-wall synthesis and PG labeling*

Fosfomycin and bacitracin were used to inhibit cell-wall synthesis. Cells were grown until exponential phase and then incubated in CH medium containing fosfomycin (final concentration 500 μg/ml) or bacitracin (final concentration 500 μg/ml) for 20 min at 30°C. To check if cell-wall synthesis was inhibited, cells were labeled with Van-FL or HADA and then imaged. Labeling with Van-FL was performed by incubating the cells with a mixture of 1:1 vancomycin (Sigma-Aldrich) and BODIPY® FL Vancomycin (Molecular Probes, Life Technologies) at a final concentration of 1 μg/ml, for 5 min at 30°C. For HADA labeling, cells were incubated with HADA (final concentration 0.5 mM) for 5 min at 30°C. Excess label was removed by three washes with Phosphate-Buffered Saline (PBS, 58 mM $Na_2HPO_4$; 17 mM $NaH_2PO_4$; 68 mM NaCl, pH 7.3). A reverse experiment was performed, in which cells were grown until exponential phase and labeled with HADA (final concentration 0.5 mM) for 5 min at 30°C. Cells were then washed three times in PBS and incubated in CH medium (either with or without bacitracin at 500 μg/ml) for an additional 20 min.

### *Sacculi isolation*

Sacculi were purified according to (Atrih *et al*., 1999) with some modifications. *B. subtilis* 168 was grown until exponential phase, boiled for 7 min and collected by centrifugation. Cells were resuspended in sodium dodecyl sulfate (SDS, 5% w/v) and boiled for 25 min. The insoluble material was recovered by centrifugation and boiled in SDS (4% w/v) for 15 min. The insoluble material was washed five times in hot

**Table 1.** Strains used in this study.

| Strain/plasmid | Genotype | Source/construction |
|---|---|---|
| ***Bacillus subtilis*** | | |
| 168 | *trpC2* | Laboratory collection |
| PY79 | Prototrophic derivative of *B. subtilis* 168 | Laboratory collection |
| 3122 | *trpC2 pbpB::pSG5061 (cat Pxyl-gfp-pbpB1-825)* | (Scheffers *et al.*, 2004) |
| 3295 | *trpC2 chr::$P_{spac}$-pbpB neo* | (Hamoen and Errington, 2003) |
| 4055 | *trpC2 amyE::spc $P_{hyperspac}$-ftsZ-eyfp* | (Krol *et al.*, 2015) |
| DK654 | *dacA::kan, in B. subtilis 3610* | gift from D. Kearns |
| 4056 | *dacA::kan, in B. subtilis 168* | this work |
| 4132 (*gfp-pbpB*) | *trpC2 chr::$P_{spac}$-pbpB neo amyE::pDMA001(spc Pxyl-gfpmut-pbpB)* | pDMA001→3295 |
| 4133 (*gfp-pbpBΔPASTA*) | *trpC2 chr::$P_{spac}$-pbpB neo amyE::pDMA002(spc Pxyl-gfpmut-pbpB$^{1-1991}$)* | pDMA002→3295 |
| 4134 (*gfp-pbpBSer312Ala*) | *trpC2 chr::$P_{spac}$-pbpB neo amyE::pDMA003(spc Pxyl-gfpmut-pbpB-T934G)* | pDMA003→3295 |
| 4135 (*gfp-pbpBSer312Ala-ΔPASTA*) | *trpC2 chr::$P_{spac}$-pbpB neo amyE::pDMA004(spc Pxyl-gfpmut-pbpB$^{1-1991}$- T934G)* | pDMA004→3295 |
| 4136 (gfp-*pbpB-supertruncated*) | *trpC2 chr::$P_{spac}$-pbpB neo amyE::pDMA005(spc Pxyl-gfpmut-pbpB-* G676A*)* | pDMA005→3295 |
| 4137 (*pbpB*) | *trpC2 chr::$P_{spac}$-pbpB neo amyE::pDMA006(spc Pxyl-pbpB)* | pDMA006→3295 |
| 4138 (*pbpBΔPASTA*) | *trpC2 chr::$P_{spac}$-pbpB neo amyE::pDMA007(spc Pxyl-pbpB$^{1-1991}$)* | pDMA007→3295 |
| 4139 (*pbpBSer312Ala*) | *trpC2 chr::$P_{spac}$-pbpB neo amyE::pDMA008(spc Pxyl-pbpB- T934G)* | pDMA008→3295 |
| 4140 (*pbpBSer312Ala-ΔPASTA*) | *trpC2 chr::$P_{spac}$-pbpB neo amyE::pDMA009(spc Pxyl-pbpB$^{1-1991-}$ T934G)* | pDMA009→3295 |
| 4141 (*pbpB-supertruncated*) | *trpC2 chr::$P_{spac}$-pbpB neo amyE::pDMA010(spc Pxyl- pbpB* G676A*)* | pDMA010→3295 |
| 4142 | *gpsB::kan* | 4221 (Claessen *et al.*, 2008) →168 |
| 4143 | *ezrA::spec* | Dennis Claessen, unpublished. |
| 4144 | *gpsB:: kan, ezrA::spec* | 4142 → 4143 |
| 4145 | *trpC2 pbpD::erm* | Dockerty *et al.*, unpublished. |
| ***Escherichia coli*** | | |
| *E. coli* MG1655 | *F-, lambda-, rph-1* | Laboratory collection |
| *E. coli* MC4100 | *F-, [araD139]B/r, Del(argF-lac)169, lambda-, e14-, flhD5301, Δ(fruK-yeiR)725(fruA25), relA1, rpsL150(strR), rbsR22, Del(fimB-fimE)632(::IS1), deoC1* | Laboratory collection |
| **Plasmids** | | |
| pSG1729 | *bla amyE3′ spc Pxyl–gfpmut1′ amyE5′* | (Lewis and Marston, 1999) |
| pGEM-T | vector for subcloning PCR products | Promega |
| pDMA001 | *bla amyE3′ spc Pxyl– pbpB gfpmut1′ amyE5′* | This work |
| pDMA002 | *bla amyE3′ spc Pxyl– pbpB$^{1991-}$ gfpmut1′ amyE5′* | This work |
| pDMA003 | *bla amyE3′ spc Pxyl–pbpB- T934G- gfpmut1′ amyE5′* | This work |
| pDMA004 | *bla amyE3′ spc Pxyl– pbpB$^{1-1991}$- T934G- gfpmut1′ amyE5′* | This work |
| pDMA005 | *bla amyE3′ spc Pxyl– pbpB-* G676A *-gfpmut1′ amyE5′* | This work |
| pDMA006 | *bla amyE3′ spc Pxyl– pbpB- amyE5′* | This work |
| pDMA007 | *bla amyE3′ spc Pxyl– pbpB$^{1991}$ amyE5′* | This work |
| pDMA008 | *bla amyE3′ spc Pxyl– pbpB- T934G amyE5′* | This work |
| pDMA009 | *bla amyE3′ spc Pxyl– pbpB$^{1-1991}$- T934G amyE5′* | This work |
| pDMA010 | *bla amyE3′ spc Pxyl– pbpB-* G676A *amyE5′* | This work |

water to remove the SDS. Sacculi were digested with 100 μg/ml amylase (*Bacillus licheniformis* type XII-A in 10 mM Tris-HCl [pH 7.0], 10 mM NaCl, 0.32 M imidazol) for 2 h at 37°C and further resuspended in sodium phosphate buffer (50 mM, pH 7.3) containing 100 μg/mL α-chymotrypsin and incubated overnight at 37°C. Sacculi were washed with water and resuspended in hydrofluoric acid (48% vol/vol) for 24 h at 4°C. Finally, sacculi were washed with Tris-HCl (50 mM, pH7) and cold water until pH was 7.

For HPLC analysis, chymotrypsin treated sacculi were extensively washed with water, resuspended in buffer (50 mM MES, 1 mM $MgCl_2$, pH 6.0) to 16.6 mg/ml and 200 μl of the sacculi were digested overnight at 37°C with mutanolysin (50 μg/ml) under constantly shaking. Samples were centrifuged for 10 min at 17,000 g and 50 μl of supernatant was analyzed by HPLC on a C18 column (HyperClone™ 5 μm ODS (C18) 120 Å, LC column 250 × 4 mm, 00G-4361-D0 from Phenomenex). The following 290-min-gradient program at a flow rate of 0.5 ml/min was used. Five minutes of washing with 100% buffer A (40 mM sodium phosphate (pH 4.5)) was followed by a linear gradient over 270 min from 0% to 100% buffer B (40 mM sodium phosphate (pH 4) containing 20% (vol/vol) methanol). A 5-min delay and 10 min of re-equilibration with buffer A completed the method.

Elution profiles were monitored by detecting UV absorbance at 202 nm and fluorescence with excitation/emission at 405/450 nm. Chromatograms were presented in the GraphPad Prism 6 program.

### *Bacterial viability*

Bacterial viability after antibiotic treatment was determined by two different assays: the live/dead bacterial viability assay and 10-fold dilution series.

Live/dead assay (Life technology) discriminates between cells with or without a compromised membrane using two DNA dyes: the membrane permeable SYTO9 dyes and membrane impermeable propidium iodide. Exponentially growing bacteria were mixed with SYTO 9 dye (0.877 μM), propidium iodide (7.5 μM) and the corresponding antibiotic to be tested (final concentration: fosfomycin 500 μg/ml, bacitracin 500 μg/ml and D-cycloserine 500 μg/ml). Cells were incubated at 30°C or 37°C (see above). Viability of cells was monitored by microscopy at 20 min and 1 h after antibiotic treatment. Pictures were taken using FITC and TRITC filters.

For the 10-fold dilution series, bacteria were grown as described above and diluted to $OD_{600}$ 0.4. The corresponding antibiotic (final concentration: fosfomycin 500 μg/ml, bacitracin 500 μg/ml and D-cycloserine 500 μg/ml) was added to the bacteria and cells were further grown for 20 min and 1 h. After this time, the bacteria were rapidly diluted in growth medium in a ten-fold dilution series and 2 μl of each dilution was plated on LB agar. Plates were incubated at 37°C overnight.

### *Fluorescence microscopy*

Cells or sacculi were spotted on agarose (1% w/v in PBS) pads and imaged using a Nikon Ti-E microscope (Nikon Instruments, Tokyo, Japan) equipped with a Hamamatsu Orca Flash4.0 camera. Image analysis was performed using the software packages ImageJ (http://rsb.info.nih.gov/ij/), ObjectJ (https://sils.fnwi.uva.nl/bcb/objectj/index.html) and Adobe Photoshop (Adobe Systems Inc., San Jose, CA, USA).

### *Time-lapse and 3D reconstruction*

Time-lapse microscopy was performed as described previously (de Jong *et al.*, 2011) using an DV Elite, IX71 (Olympus, Japan) microscope with a sCMOS camera assembled by Applied Precision (GE Healthcare), with laser excitation at 405 nm (laser power 20%) and a CFP filter. Pictures were taken every 5 min.

Z-stacks were captured with steps of 0.08 μm on the same microscope setup. Deconvolution and 3D reconstruction was performed using Deltavision's Softworx software (Applied Precision).

## Acknowledgements

We would like to thank Michael Van Nieuwenzhe, Yves Brun and Erkin Kuru (Indiana University, Bloomington, USA) for sending us an initial stock of HADA and detailed protocols for synthesis. We would like to thank Avatar Joshi and Daniel Kearns (Indiana University, Bloomington, USA) for sending strain DK654, and Dennis Claessen (Leiden University, NL) for strains 4221 and 4143. We thank Oguz Bolgi and Alexander Schneider for technical assistance.

Work in the Scheffers lab is supported by a VIDI fellowship (864.09.010) from the Netherlands Organisation for Scientific Research. Work in the Veening lab is supported by the EMBO Young Investigator Program, a VIDI fellowship (864.12.001) from the Netherlands Organisation for Scientific Research, and ERC starting grant 337399-PneumoCell. Yun Liu was supported by a PhD fellowship from the Chinese Scholarship Council, and Anabela de Sousa Borges was supported by a doctoral grant (SFRH/BD/78061/2011) from POPH/FSE and FCT (Fundação para a Ciência e Tecnologia) from Portugal. Work in the Hirsch lab is supported by funding from the Dutch Ministry of Education, Culture and Science (Gravitation program 024.001.035) and a VIDI grant (723.014.008) from the Netherlands Organisation for Scientific Research (NWO-CW).

## Author Contributions

The conception or design of the study: DMA, DJS.

The acquisition, analysis, or interpretation of the data: DMA, YL, AMH, MB, ASB, NdK, KB, JWV, CM, AKHH, DJS

Writing of the manuscript: DMA, ASB, JWV, AKHH, DJS.

## References

Anagnostopoulos, C., and Spizizen, J. (1961) Requirements for transformation in Bacillus subtilis. *J Bacteriol* **81**: 741–746.

Atrih, A., Bacher, G., Allmaier, G., Williamson, M.P., and Foster, S.J. (1999) Analysis of peptidoglycan structure from vegetative cells of Bacillus subtilis 168 and role of PBP 5 in peptidoglycan maturation. *J Bacteriol* **181**: 3956–3966.

Boersma, M.J., Kuru, E., Rittichier, J.T., VanNieuwenhze, M.S., Brun, Y.V., and Winkler, M.E. (2015) Minimal Peptidoglycan (PG) turnover in wild-type and pg hydrolase and cell division mutants of streptococcus pneumoniae D39 growing planktonically and in host-relevant biofilms. *J Bacteriol* **197**: 3472–3485.

Burdett, I.D., and Higgins, M.L. (1978) Study of pole assembly in Bacillus subtilis by computer reconstruction of septal growth zones seen in central, longitudinal thin sections of cells. *J Bacteriol* **133**: 959–971.

Cameron, T.A., Zupan, J.R., and Zambryski, P.C. (2015) The essential features and modes of bacterial polar growth. *Trends Microbiol* **23**: 347–353.

Cava, F., de Pedro, M.A., Lam, H., Davis, B.M., and Waldor, M.K. (2011) Distinct pathways for modification of the bacterial cell wall by non-canonical D-amino acids. *EMBO J* **30**: 3442–3453.

Cho, H., Wivagg, C.N., Kapoor, M., Barry, Z., Rohs, P.D., Suh, H., *et al.* (2016) Bacterial cell wall biogenesis is mediated by SEDS and PBP polymerase families functioning semi-autonomously. *Nat Microbiol* 16172.

Claessen, D., Emmins, R., Hamoen, L.W., Daniel, R.A., Errington, J., and Edwards, D.H. (2008) Control of the cell elongation-division cycle by shuttling of PBP1 protein in Bacillus subtilis. *Mol Microbiol* **68**: 1029–1046.

Clarke-Sturman, A.J., Archibald, A.R., Hancock, I.C., Harwood, C.R., Merad, T., and Hobot, J.A. (1989) Cell wall assembly in Bacillus subtilis: partial conservation of polar wall material and the effect of growth conditions on the pattern of incorporation of new material at the polar caps. *J Gen Microbiol* **135**: 657–665.

Daniel, R.A., and Errington, J. (2003) Control of cell morphogenesis in bacteria: Two distinct ways to make a rod-shaped cell. *Cell* **113**: 767–776.

Daniel, R.A., Williams, A.M., and Errington, J. (1996) A complex four-gene operon containing essential cell division gene pbpB in Bacillus subtilis. *J Bacteriol* **178**: 2343–2350.

Daniel, R.A., Harry, E.J., and Errington, J. (2000) Role of penicillin-binding protein PBP 2B in assembly and functioning of the division machinery of Bacillus subtilis. *Mol Microbiol* **35**: 299–311.

de Jong, I.G., Beilharz, K., Kuipers, O.P., and Veening, J.W. (2011) Live Cell Imaging of Bacillus subtilis and Streptococcus pneumoniae using Automated Time-lapse Microscopy. *J Vis Exp* **28**: 3145.

de Jonge, B.L., Chang, Y.S., Gage, D., and Tomasz, A. (1992) Peptidoglycan composition in heterogeneous Tn551 mutants of a methicillin-resistant Staphylococcus aureus strain. *J Biol Chem* **267**: 11255–11259.

de Pedro, M.A., and Cava, F. (2015) Structural constraints and dynamics of bacterial cell wall architecture. *Front Microbiol* **6**: 449.

de Pedro, M.A., Quintela, J.C., Höltje, J.V., and Schwarz, H. (1997) Murein segregation in Escherichia coli. *J Bacteriol* **179**: 2823–2834.

de Pedro, M.A., Young, K.D., Holtje, J.V., and Schwarz, H. (2003) Branching of Escherichia coli cells arises from multiple sites of inert peptidoglycan. *J Bacteriol* **185**: 1147–1152.

Dominguez-Escobar, J., Chastanet, A., Crevenna, A.H., Fromion, V., Wedlich-Soldner, R., and Carballido-Lopez, R. (2011) Processive movement of MreB-associated cell wall biosynthetic complexes in bacteria. *Science* **333**: 225–228.

Errington, J., Daniel, R.A., and Scheffers, D.J. (2003) Cytokinesis in bacteria. *Microbiol Mol Biol Rev* **67**: 52–65.

Fura, J.M., Kearns, D., and Pires, M.M. (2015) D-Amino acid probes for penicillin binding protein-based bacterial surface labeling. *J Biol Chem* **290**: 30540–30550.

Garner, E.C., Bernard, R., Wang, W., Zhuang, X., Rudner, D.Z., and Mitchison, T. (2011) Coupled, circumferential motions of the cell wall synthesis machinery and MreB filaments in B. subtilis. *Science* **333**: 222–225.

Gundogdu, M.E., Kawai, Y., Pavlendova, N., Ogasawara, N., Errington, J., Scheffers, D.J., and Hamoen, L.W. (2011) Large ring polymers align FtsZ polymers for normal septum formation. *EMBO J* **30**: 617–626.

Hamoen, L.W., and Errington, J. (2003) Polar targeting of DivIVA in Bacillus subtilis is not directly dependent on FtsZ or PBP 2B. *J Bacteriol* **185**: 693–697.

Harwood, C.R., and Cutting, S.M. (1990) *Molecular Biological Methods for Bacillus*. Chichester: Wiley.

Hayhurst, E.J., Kailas, L., Hobbs, J.K., and Foster, S.J. (2008) Cell wall peptidoglycan architecture in Bacillus subtilis. *Proc Natl Acad Sci USA* **105**: 14603–14608.

Höltje, J.V. (1998) Growth of the stress-bearing and shape-maintaining murein sacculus of Escherichia coli. *Microbiol Mol Biol Rev* **62**: 181–203.

Krol, E., de Sousa Borges, A., da Silva, I., Polaquini, C.R., Regasini, L.O., Ferreira, H., and Scheffers, D.J. (2015) Antibacterial activity of alkyl gallates is a combination of direct targeting of FtsZ and permeabilization of bacterial membranes. *Front Microbiol* **6**: 390.

Kuru, E., Hughes, H.V., Brown, P.J., Hall, E., Tekkam, S., Cava, F., *et al.* (2012) In Situ probing of newly synthesized peptidoglycan in live bacteria with fluorescent D-amino acids. *Angew Chem Int Ed Engl* **51**: 12519–12523.

Kuru, E., Tekkam, S., Hall, E., Brun, Y.V., and Van Nieuwenhze, M.S. (2015) Synthesis of fluorescent D-amino acids and their use for probing peptidoglycan synthesis and bacterial growth in situ. *Nat Protoc* **10**: 33–52.

Lages, M.C., Beilharz, K., Morales Angeles, D., Veening, J.W., and Scheffers, D.J. (2013) The localization of key Bacillus subtilis penicillin binding proteins during cell growth is determined by substrate availability. *Environ Microbiol* **15**: 3272–3281.

Lewis, P.J., and Marston, A.L. (1999) GFP vectors for controlled expression and dual labelling of protein fusions in Bacillus subtilis. *Gene* **227**: 101–109.

Maestro, B., Novakova, L., Hesek, D., Lee, M., Leyva, E., Mobashery, S., *et al.* (2011) Recognition of peptidoglycan and beta-lactam antibiotics by the extracellular domain of the Ser/Thr protein kinase StkP from Streptococcus pneumoniae. *FEBS Lett* **585**: 357–363.

Magnet, S., Dubost, L., Marie, A., Arthur, M., and Gutmann, L. (2008) Identification of the L, D-transpeptidases for peptidoglycan cross-linking in Escherichia coli. *J Bacteriol* **190**: 4782–4785.

Meeske, A.J., Riley, E.P., Robins, W.P., Uehara, T., Mekalanos, J.J., Kahne, D., *et al.* (2016) SEDS proteins are a widespread family of bacterial cell wall polymerases. *Nature* **537**: 634–638.

Memmi, G., Filipe, S.R., Pinho, M.G., Fu, Z., and Cheung, A. (2008) Staphylococcus aureus PBP4 is essential for beta-lactam resistance in community-acquired methicillin-resistant strains. *Antimicrob Agents Chemother* **52**: 3955–3966.

Mir, M., Asong, J., Li, X., Cardot, J., Boons, G.J., and Husson, R.N. (2011) The extracytoplasmic domain of the Mycobacterium tuberculosis Ser/Thr kinase PknB binds specific muropeptides and is required for PknB localization. *PLoS Pathog* **7**: e1002182.

Morlot, C., Noirclerc-Savoye, M., Zapun, A., Dideberg, O., and Vernet, T. (2004) The carboxypeptidase PBP3 organizes the division process of Streptococcus pneumoniae. *Mol Microbiol* **51**: 1641–1648.

Morlot, C., Bayle, L., Jacq, M., Fleurie, A., Tourcier, G., Galisson, F., *et al.* (2013) Interaction of Penicillin-Binding

Protein 2x and Ser/Thr protein kinase StkP, two key players in Streptococcus pneumoniae R6 morphogenesis. *Mol Microbiol* **90**: 88–102.
Paracuellos, P., Ballandras, A., Robert, X., Kahn, R., Herve, M., Mengin-Lecreulx, D., *et al*. (2010) The extended conformation of the 2.9-A crystal structure of the three-PASTA domain of a Ser/Thr kinase from the human pathogen Staphylococcus aureus. *J Mol Biol* **404**: 847–858.
Peters, K., Schweizer, I., Beilharz, K., Stahlmann, C., Veening, J.W., Hakenbeck, R., and Denapaite, D. (2014) Streptococcus pneumoniae PBP2x mid-cell localization requires the C-terminal PASTA domains and is essential for cell shape maintenance. *Mol Microbiol* **92**: 733–755.
Pinho, M.G., Kjos, M., and Veening, J.W. (2013) How to get (a)round: Mechanisms controlling growth and division of coccoid bacteria. *Nat Rev Microbiol* **11**: 601–614.
Potluri, L.P., de Pedro, M.A., and Young, K.D. (2012) Escherichia coli low-molecular-weight penicillin-binding proteins help orient septal FtsZ, and their absence leads to asymmetric cell division and branching. *Mol Microbiol* **84**: 203–224.
Randich, A.M., and Brun, Y.V. (2015) Molecular mechanisms for the evolution of bacterial morphologies and growth modes. *Front Microbiol* **6**: 580.
Scheffers, D.J., and Pinho, M.G. (2005) Bacterial cell wall synthesis: New insights from localization studies. *Microbiol Mol Biol Rev* **69**: 585–607.
Scheffers, D.J., Jones, L.J.F., and Errington, J. (2004) Several distinct localization patterns for penicillin-binding proteins in Bacillus subtilis. *Mol Microbiol* **51**: 749–764.
Shah, I.M., Laaberki, M.H., Popham, D.L., and Dworkin, J. (2008) A eukaryotic-like Ser/Thr kinase signals bacteria to exit dormancy in response to peptidoglycan fragments. *Cell* **135**: 486–496.
Squeglia, F., Marchetti, R., Ruggiero, A., Lanzetta, R., Marasco, D., Dworkin, J., *et al*. (2011) Chemical basis of peptidoglycan discrimination by PrkC, a key kinase involved in bacterial resuscitation from dormancy. *J Am Chem Soc* **133**: 20676–20679.
Strahl, H., and Hamoen, L.W. (2010) Membrane potential is important for bacterial cell division. *Proc Natl Acad Sci USA* **107**: 12281–12286.
Strahl, H., Burmann, F., and Hamoen, L.W. (2014) The actin homologue MreB organizes the bacterial cell membrane. *Nat Commun* **5**: 3442.
Szwedziak, P., and Lowe, J. (2013) Do the divisome and elongasome share a common evolutionary past?. *Curr Opin Microbiol* **16**: 745–751.
Tsui, H.C., Boersma, M.J., Vella, S.A., Kocaoglu, O., Kuru, E., Peceny, J.K., *et al*. (2014) Pbp2x localizes separately from Pbp2b and other peptidoglycan synthesis proteins during later stages of cell division of Streptococcus pneumoniae D39. *Mol Microbiol* **94**: 21–40.
Turner, R.D., Vollmer, W., and Foster, S.J. (2014) Different walls for rods and balls: The diversity of peptidoglycan. *Mol Microbiol* **91**: 862–874.
Typas, A., Banzhaf, M., Gross, C.A., and Vollmer, W. (2012) From the regulation of peptidoglycan synthesis to bacterial growth and morphology. *Nat Rev Microbiol* **10**: 123–136.
Varma, A., and Young, K.D. (2004) FtsZ collaborates with penicillin binding proteins to generate bacterial cell shape in Escherichia coli. *J Bacteriol* **186**: 6768–6774.
Yahashiri, A., Jorgenson, M.A., and Weiss, D.S. (2015) Bacterial SPOR domains are recruited to septal peptidoglycan by binding to glycan strands that lack stem peptides. *Proc Natl Acad Sci USA* **112**: 11347–11352.

## Supporting information

Additional supporting information may be found in the online version of this article at the publisher's web-site.